Using global tide gauge data to validate and improve the representation of extreme sea levels in flood impact studies

J.R. Hunter[a], P.L. Woodworth[b,*], T. Wahl[c], R.J. Nicholls[d]

[a] Antarctic Climate & Ecosystems Cooperative Research Centre, University of Tasmania, Private Bag 80, Hobart, Tasmania 7001, Australia
[b] National Oceanography Centre, Joseph Proudman Building, 6 Brownlow Street, Liverpool L3 5DA, United Kingdom
[c] Department of Civil, Environmental and Construction Engineering and Sustainable Coastal Systems Cluster, University of Central Florida, 12800 Pegasus Drive, Orlando 32816-2450, USA
[d] Faculty of Engineering and the Environment, University of Southampton, Southampton SO17 1BJ, United Kingdom

ARTICLE INFO

ABSTRACT

The largest collection of tide gauge records assembled to date, called GESLA-2, has been used to provide reliable extreme sea level parameters at 655 locations around the world. This has enabled a rigorous assessment of the European Union-funded DINAS-COAST (D-C) data set of extreme sea level information for the global coastline that has been used in many published flood impact studies. We find the D-C extreme levels to be generally both too high, compared to those from GESLA-2, and too flat, when plotted as a function of return period. This leads to an over-estimation of the probability of extreme sea levels in the present day for most locations around the world, and also to an over-estimation of the probability of extreme sea levels in the future as sea level rises. A detailed impact study is conducted for the world's largest coastal cities following the approach of Hallegatte et al. (2013), resulting in similar conclusions for these particular locations. We suggest that most previous studies that have relied upon D-C information should be re-assessed in the light of these findings, using more recent modelling-based estimates of extreme sea level information.

1. Introduction

As climate changes, and as sea level rises, coastal impacts are expected due to an increase in the likelihood of flooding. There will be costs associated with flood damage, human impacts and the need for modified coastal infrastructure and adaptation. Such impacts have been assessed at local to global scales using knowledge of the distribution of coastal populations and assets, coastal topography, estimates of present and future coastal adaptation, and plausible projections of future increases in mean and extreme sea levels (Nicholls, 2010). Extreme level parameters are needed in such studies in order to estimate present-day and future changes in the likelihood of extreme events as sea level rises.

A notable achievement in this area of research has been the development of the Dynamic and Interactive Vulnerability Assessment (DIVA) model (Hinkel and Klein, 2009; Hinkel et al., 2014) which has been employed to estimate the global costs of coastal impacts under scenarios of climate, sea level and socio-economic change, and has been influential in review processes such as the Intergovernmental Panel on Climate Change Fifth Assessment Report (IPCC AR5). The parameterisation of the likelihood of extreme sea levels used in most DIVA assessments was developed more than a decade ago by the European

Union (EU)-funded DINAS-COAST (Dynamic and Interactive Assessment of National, Regional and Global Vulnerability of Coastal Zones to Sea-Level Rise, hereafter D-C) project (Vafeidis et al., 2008).

In this paper, we report on a rigorous assessment of the extreme level parameterisations in D-C by means of an independent quasi-global data set of extreme sea level information obtained by tide gauges. This tide gauge data set is the largest ever to have been assembled. For each tide gauge record spanning at least 20 years, we have computed extreme sea level parameters, suitable for comparison to those in D-C at the same locations, and thereby providing as complete as possible a validation of the D-C data set.

This assessment demonstrates that there are important deficiencies in the D-C data, as might be expected in a relatively old dataset. Nevertheless, we feel that it is useful to clarify these deficiencies as the D-C data has been used extensively in earlier impact and adaptation research of coasts (e.g. McLeod et al., 2010; Hanson et al., 2011; Nicholls et al., 2011; Pardaens et al., 2011; Bosello et al., 2012; Hallegatte et al., 2013; Hinkel et al., 2010, 2014; Brown et al., 2016; Diaz, 2016), including in the IPCC AR5 Working Group II (Wong et al., 2014).

There is particular interest in knowing how coastal cities around the

world may be subject to a greater frequency of flooding as sea level rises as they represent impact (and adaptation) hotspots. Many of these cities have tide gauges nearby which have long records from which reliable extreme sea level information may be extracted. We have used a flood risk model developed by Hallegatte et al. (2013) to explore how improved estimates of extreme sea levels from these tide gauges, instead of D-C information, change exposure and risk estimates at these locations for the present-day and with future sea level rise.

In Section 2 below, we describe how extreme sea levels recorded by tide gauges are usually parameterised as either Generalised Extreme Value (GEV) or the more restrictive Gumbel distributions, and how parameters from the latter can be used to determine 1, 10, 100 and 1000 year return levels for comparison with the information in D-C. We then provide some background to the development of the D-C data set and describe briefly how extreme sea level information is parameterised within it. That is followed by an introduction to the quasi-global tide gauge data set called GESLA-2 that we have used to validate the D-C values. Section 3 describes our main findings from comparisons of D-C and GESLA-2 information. Section 4 then considers how different estimates of changes in flood risk pertain to coastal cities, using either the D-C or GESLA-2 information. Section 5 refers to the implications for changes in the frequency of extreme sea levels with sea level rise, and finally Section 6 summarises our conclusions.

2. Extreme levels and data sets

2.1. Extreme level distributions

The highest sea level (also called the extreme sea level) recorded by a tide gauge in a year will vary from year to year due to many factors. These factors include interannual changes in the ocean tide, variations in the occurrence of large storm surges due to both tropical and extratropical cyclones (e.g. von Storch and Woth, 2008; Khouakhi and Villarini, 2016), and fluctuations in mean sea level (MSL) such as those that can be many decimetres in magnitude that occur in the tropical Pacific during El Niño Southern Oscillation (ENSO) events (Merrifield et al., 2013). The likelihood of a particular extreme level is commonly parameterised as a GEV distribution containing three parameters: the location, scale and shape parameters. The location parameter represents the height for some specific return period (e.g. the 1-year return level), the scale parameter gives the spread of extreme values from year to year (an e-folding distance in the vertical), and the shape parameter determines the upper tail of the distribution and describes the behaviour of the most unusual extreme events (Pugh and Woodworth, 2014). When the shape parameter is taken as zero, the GEV is reduced to a Gumbel distribution (Coles, 2001):

$$N = \frac{1}{R} = \exp((\mu - h)/\lambda) \tag{1}$$

where N is the frequency of a level h being exceeded in a given year, which corresponds to a return period R and where μ and λ are the location and scale parameters respectively (the 'return period' is also called the 'average recurrence interval'). In most cases, the Gumbel distribution is found to be an adequate approximation of the GEV for return periods of 10s to 100s of years, i.e. for almost all observed extremes except for the most rare events (e.g. van den Brink and Können, 2011). Pairs of the 1, 10, 100 and 1000 year return period extreme levels above MSL ($H1$, $H10$, $H100$ and $H1000$) then have simple linear relationships such as:

$$(H100 - H1)\big/\lambda = \ln\frac{1}{1} - \ln\frac{1}{100} \tag{2}$$

where $H1$ is identical to the location parameter μ. In this situation, an 'extreme level curve', obtained by plotting extreme level versus the logarithm of the return period, is a straight line with a gradient that is proportional to the scale parameter.

This approach to our analysis of the tide gauge data from GESLA-2 is also appropriate for study of the extreme levels in the D-C data set which, it will be seen below, are largely consistent with having a Gumbel-like form for most of the world coastline.

2.2. DINAS-COAST and GESLA-2 information

The D-C data set of extreme sea level information has a heritage in the earlier studies of the Global Vulnerability Assessment (GVA) (Hoozemans et al., 1993; Nicholls and Hoozemans, 2005). In these studies, present-day extreme sea levels around the global coastline are estimated by combining information on several oceanographic processes which result in high sea levels: the range of the ocean tide at the coast as represented by values of mean high water (MHW) above MSL taken from tide tables; the frequency and magnitude of storm surge (wind setup), simply modelled from wind conditions (which are inferred in turn from statistics of the wave climate) and estimates of the bottom slope and depth; and the possible changes in barometric pressure during storms. Other oceanographic processes, such as variability in the ocean circulation, are not included. This information on sea level variability is then used to derive present-day extreme sea level parameters, which are then combined with estimates of coastal subsidence and projections of MSL change in order to perform an impact assessment for some time in the future.

The D-C data set consists of a table of values of 1, 10, 100 and 1000 year extreme levels above MSL (i.e. the $H1$, $H10$, $H100$ and $H1000$ quantities mentioned above) for 12,148 segments of the world coastline excluding Antarctica (Vafeidis et al., 2008; Wolff et al., 2016). The median distance between nearest-neighbour segment centroids is 10.5 km. Pairs of H values can be used to determine the equivalent scale parameters according to Eq. (2). In the results shown below, we have made use of $H1$ and $H100$ finding little difference when using $H10$ and $H1000$ (see below).

The tide gauge information comes from a data set called GESLA-2 that has been assembled from a number of national and international sea level databanks by Philip Woodworth (National Oceanography Centre, UK), John Hunter (University of Tasmania, Australia), Marta Marcos (University of the Balearic Islands, Spain), Melisa Menéndez (University of Cantabria, Spain) and Ivan Haigh (University of Southampton, UK). It is an update and extension of the GESLA (Global Extreme Sea Level Analysis) data set used by Menéndez and Woodworth (2010) and others. Although there are many individual contributions to GESLA-2, well over a quarter of its station-years are provided by the research quality data set of the University of Hawaii Sea Level Center. The GESLA-2 data set already has a reasonable geographical distribution (Fig. SM1), although some coastline stretches have little or no coverage. It is planned to add other data in the future as it becomes available.

The data set presently contains 39,151 station-years of information from 1355 station records (with some stations having alternative versions of the records provided by different sources) or typically 29 years per record, although the actual number of years varies from only 1 at several short-lived sites, to 167 in the case of Brest, France. The data set may be obtained from www.gesla.org. More detailed information may be found in Woodworth et al. (2017).

All the tide gauge data in GESLA-2 have hourly or more frequent sampling. Records will have had some form of quality control undertaken by the data providers. However, the extent to which that control will have been undertaken will inevitably vary between providers and probably with time. We are interested in non-tsunami ocean processes for comparison with D-C information. However, while some large tsunami signals and other data 'spikes' will have been removed from, or flagged in, the tide-gauge records, some will undoubtedly remain. Therefore, in the first procedure to be described (the one that is used for the final analyses), we apply a simple method for the rejection of outlier annual maxima. We believe that the resultant extremes parameters are

adequate for making regional comparisons with D-C information. (There is a general question to do with the analysis of extreme sea levels from tide gauge records, as to whether the most extreme events are reliably recorded, see for example Section 7.3 of Pugh and Woodworth (2014). However, any locations where there is significant loss of data on the highest extremes would likely yield extremes distributions that are significantly non-Gumbel, leading to rejection by our iterative quality control procedure. In the present application of the data set, which involves validation of the D-C data set on a regional and global basis, we do not believe this question to be of major importance.)

We use annual extreme sea levels from the tide gauge records in GESLA-2. These extreme values are the overall observed ones i.e. we are not concerned if the extremes arise primarily from variations in the tide or in 'surge' or 'mean sea level' components. Gumbel parameters were computed from the observed extremes by two methods.

The first method is based on that described by Hunter (2012). Prior to extremes analysis, the data were detrended, and then 'binned' so as to produce files with a minimum sampling interval of 1 h. Annual maxima were estimated using a declustering algorithm such that any extreme events closer than 3 days were counted as a single event, and any gaps in time were removed from the record. The method fits these annual maxima to a Gumbel distribution using the *ismev* package (Coles, 2001, p. 48) implemented in the statistical language R (R Development Core Team, 2011). Annual maxima were then rejected in an iterative fashion (with a maximum of 5 iterations) if they fell outside a specified range (roughly 3.2-sigma) based on the estimated uncertainty range of the Gumbel fit and the number of annual maxima (each time revising the earlier detrending process using the reduced data set). If this process removed more than 15% of the original annual maxima, that tide gauge record was not used. In addition, we removed four more records (from Balboa, Newlyn, Brest and Roscoff) as further inspection showed the distribution of their extremes to be clearly non-Gumbel in character. Records that survived these tests were assumed to have an effective length equal to the number of annual maxima used in the final Gumbel fit.

Fig. 1 provides examples of linear Gumbel fits using this procedure for six stations in quite different locations. In each case, it shows annual maximum sea levels (above MSL) plotted versus return period with the dashed lines giving 95% confidence intervals. The black squares are the corresponding $H1$, $H10$ and $H100$ values (above MSL) for each location in the D-C data set, several of which will be referred to below.

The number of annual maxima used in the final Gumbel fits is shown in Fig. 2, and for further analysis we require that this value be at least 20 years resulting in 655 stations. Fig. 2 shows that in most cases there are less than 60 annual maxima, although there is a long tail, with a largest value of 123 years in the record from Stockholm, Sweden. (Brest does not provide our longest record for analysis as many of its years of data are rejected in the above procedure.) Some of the peaks in this distribution are artefacts of contributions to GESLA-2 from authorities with a large number of stations, with each of their records spanning a similar period. For example, of the 27 stations in the peak at 44 years, 11 are from Finland. The group with records of 60–65 years is primarily from the USA.

It is generally accepted that return periods may be extrapolated out to around four times the number of available annual maxima (see, for example, Pugh and Woodworth, 2014, page 323). We have checked that the Gumbel fits provide formal errors which are consistent with this expectation. We find the average errors (95% confidence level) of the 100-year return period levels to be ~0.15 m (7.2% of the levels themselves expressed relative to MSL) using the whole data set (655 stations), or a little larger (~0.17 m or 8.1%) for the 225 stations with only 20–30 annual maxima. This confirms that the fits have value out to return periods of approximately a century, which is our main timescale of interest.

A second method made use of independent software to obtain annual maximum sea level from each year of data that was at least 75%

complete. Care was taken not to include two annual maxima occurring within a 3-day window at calendar year end/start. In these cases, the smaller of the two maxima was excluded and an iterative search made for annual maxima at least 3 days apart in the two individual years. Annual maxima were then expressed relative to the MSL linear trend for the same years of data, so as to remove long-term changes in sea and land levels, in order to obtain extremes relative to an "MSL datum" that is more akin to that implied in the D-C information. The Gumbel parameters were then determined using the Matlab® *evfit* function.

The two methods resulted in almost the same Gumbel parameters and for the present study we have used values from the first method only. The Gumbel location and scale parameters from that method and their uncertainties are given in the Supplementary Material.

3. Comparisons of D-C and GESLA-2 information

Fig. 3(a) shows the extreme level information for the world coastline in the D-C data set. It shows the distribution of the reciprocals of the scale parameters at each coastal location, as calculated from the $H1$ and $H100$ levels and using Eq. (2). (An exponential of the reciprocal of the scale parameter determines the increase in the frequency of exceeding a given level using a Gumbel distribution, as discussed further below.) These scale parameters are about 13% smaller than those using $H10$ and $H1000$ (Fig. SM2) which suggests that the D-C H values are not completely linear (or Gumbel-like) but bend upwards at higher return periods (i.e. in a GEV there would be a small positive shape parameter, see Coles (2001, p.50)). However, this 13% effect is not sufficiently large so as to invalidate our use of Gumbel parameterisations in the present analysis.

Most of the coastline in Fig. 3(a) can be seen to be coloured red (i.e. the scale parameters at these locations are of the order of 0.05 m or less), although some sections of coast including NW Europe, the Atlantic coast of N America and the Russian Arctic are blue (i.e. scale parameters typically 0.2 m).

For comparison, Fig. 3(b) shows the reciprocals of the scale parameters for the 655 stations in the GESLA-2 data set that have at least 20 years of data. Although GESLA-2 does not extend to the entire global coastline, unlike D-C, there are sufficient points at which to perform a validation of the D-C information.

There can be seen to be some similarities between Fig. 3(a) and (b), such as the sections of coast in blue for NW Europe and the Atlantic and Gulf coasts of N America. However, there are also differences, such as the Pacific coasts of N and S America which are all red in Fig. 3(a), but are blue along the Canadian and Alaskan coasts in Fig. 3(b). In addition, on the coasts of Australia and China there are generally more (and darker) blue dots in panel (b) than in (a).

In spite of the spatial limitations of the GESLA-2 data set, it has sufficient coverage to make a first general point: that the D-C data set contains scale parameters that are generally too small, or, in other words, contains sets of extreme level information ($H1$, $H10$, $H100$ and $H1000$) that describe return level curves (plots of extreme level versus the logarithm of the return period) that have too small a gradient (i.e. they are too 'flat', such as for Sitka, Aburatsu and Stockholm in Fig. 1).

Figs. 4 and 5 show comparisons between the two data sets using values from GESLA-2 and their nearest D-C locations. A maximum separation of 170 km between the centroid of a D-C segment and the tide gauge in GESLA-2 was allowed, which removed 26 of the 655 GESLA-2 records, and left 629 records. As mentioned above, the D-C segment centroids are mostly spaced apart by ~10 km. The 170 km separation cut was designed to exclude remote stations which are not represented in the D-C data such as Antarctica and some remote islands.

Fig. 4(a) shows a scatter plot of GESLA-2 vs. D-C scale parameters. Their differences have a median of 0.024 m and a standard deviation of 0.071 m (Fig. 4b). The distribution is best described by the dashed line representing a least-squares fit through the origin, expressing D-C scale parameters as 0.70 ± 0.02 times those from GESLA-2. This confirms
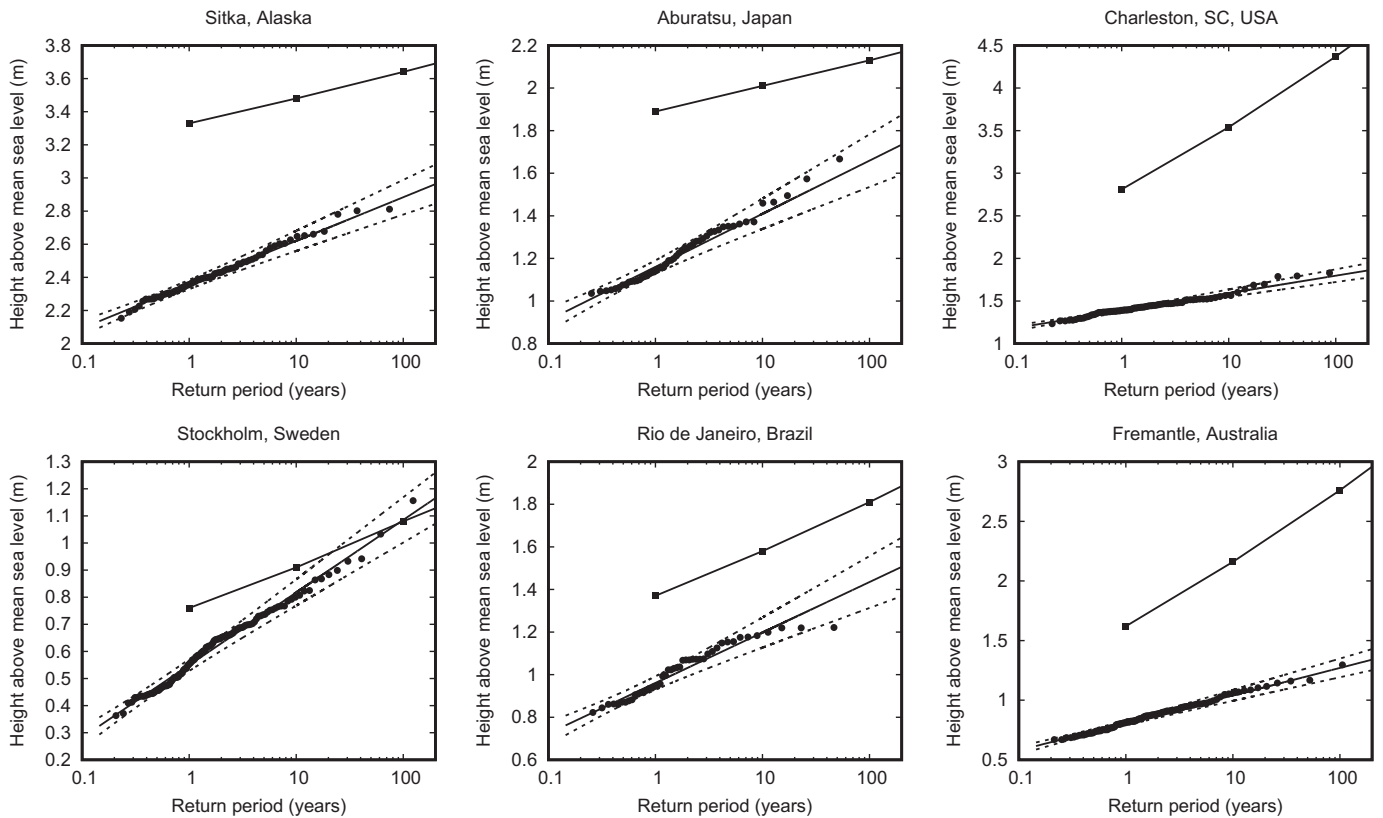
Fig. 1. Annual maximum sea levels (above MSL) plotted versus return period observed at stations in quite different locations: Sitka, Alaska, United States; Aburatsu, Japan; Charleston, South Carolina, United States; Stockholm, Sweden; Isla Fiscal, Rio de Janeiro, Brazil; Fremantle, Australia. The dashed lines give 95% confidence intervals for the linear Gumbel fits. The black squares are the $H1$, $H10$ and $H100$ values (above MSL) for this location in the D-C data set.
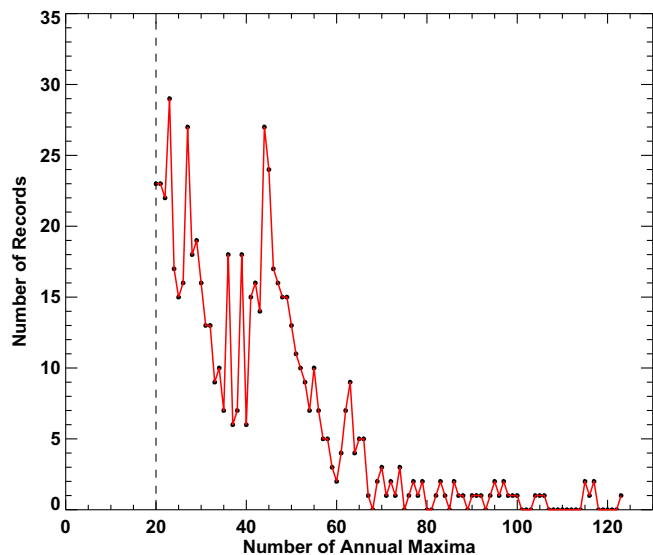

Fig. 2. Number of annual maximum sea levels used in the final Gumbel fits in method 1. Only records with more than 20 annual maxima are shown and are used in the subsequent analysis.

our impressions from inspection of Fig. 3(a) and (b): most points do not lie on the diagonal, but the true scale parameters at these locations, as provided by GESLA-2, are larger than the ones suggested by D-C. There is a very weak correlation between the two sets (correlation coefficient = 0.196), corresponding to 4% of the variance in D-C scale parameter values being explainable by the corresponding GESLA-2 values.

Fig. 5(a) addresses the same topic, but in terms of the $H1$, $H10$,

$H100$ and $H1000$ values at each location instead of scale parameters. This figure allows us to make our second general point: that the extreme levels ($H1$ to $H1000$), or the location parameters of the Gumbel distribution, in D-C are too large when compared to GESLA-2. This bias could be explained by imprecise ocean tide assumptions in D-C regarding the height of MHW above MSL, or, more likely, errors in the modelling of the surge component of the extremes.

Fig. 5(b) shows that in most cases the differences $H1000$ minus $H1$ in GESLA-2 are larger than in D-C. This relates to our first general point: that the extreme level curves in D-C are too flat, as previously demonstrated by the scale parameters in Fig. 4(a).

Similar conclusions to those obtained from Fig. 5(a, b) can be drawn from complementary cumulative distribution function (CCDF, also sometimes called the 'exceedance distribution') curves of $H1$ etc. from the available sets of D-C and GESLA-2 information. Fig. 5(c) shows the D-C CCDF curves for $H1$, $H10$, $H100$ and $H1000$ by lines in green, blue, red and black respectively. To their left, can be seen the set of four curves for GESLA-2, similarly coloured. For example, the black curve for D-C indicates that $H1000$ exceeds 4 m (above MSL) at approximately 20% of stations. On the other hand, the corresponding GESLA-2 black curve indicates that 20% of stations have values of $H1000$ exceeding only 3 m. Fig. 5(c) can be inspected further to measure the spread of the $H1$–$H1000$ curves at their mid-points where the CCDF value is 0.5. The spread between the D-C distributions (green to black lines) at this mid-point is 0.59 m. This spread is more than 25% less than that in the GESLA-2 distributions (green to black lines) which is 0.80 m.

The same conclusions obtained from Figs. 4 and 5 are found by requiring the GESLA-2 records to have at least 30 years of data rather than 20 years; in this case, 446 records are available, of which 435 remain after the 170 km separation requirement. The median difference between the two is 0.027 m, with a standard deviation of 0.069 m and a
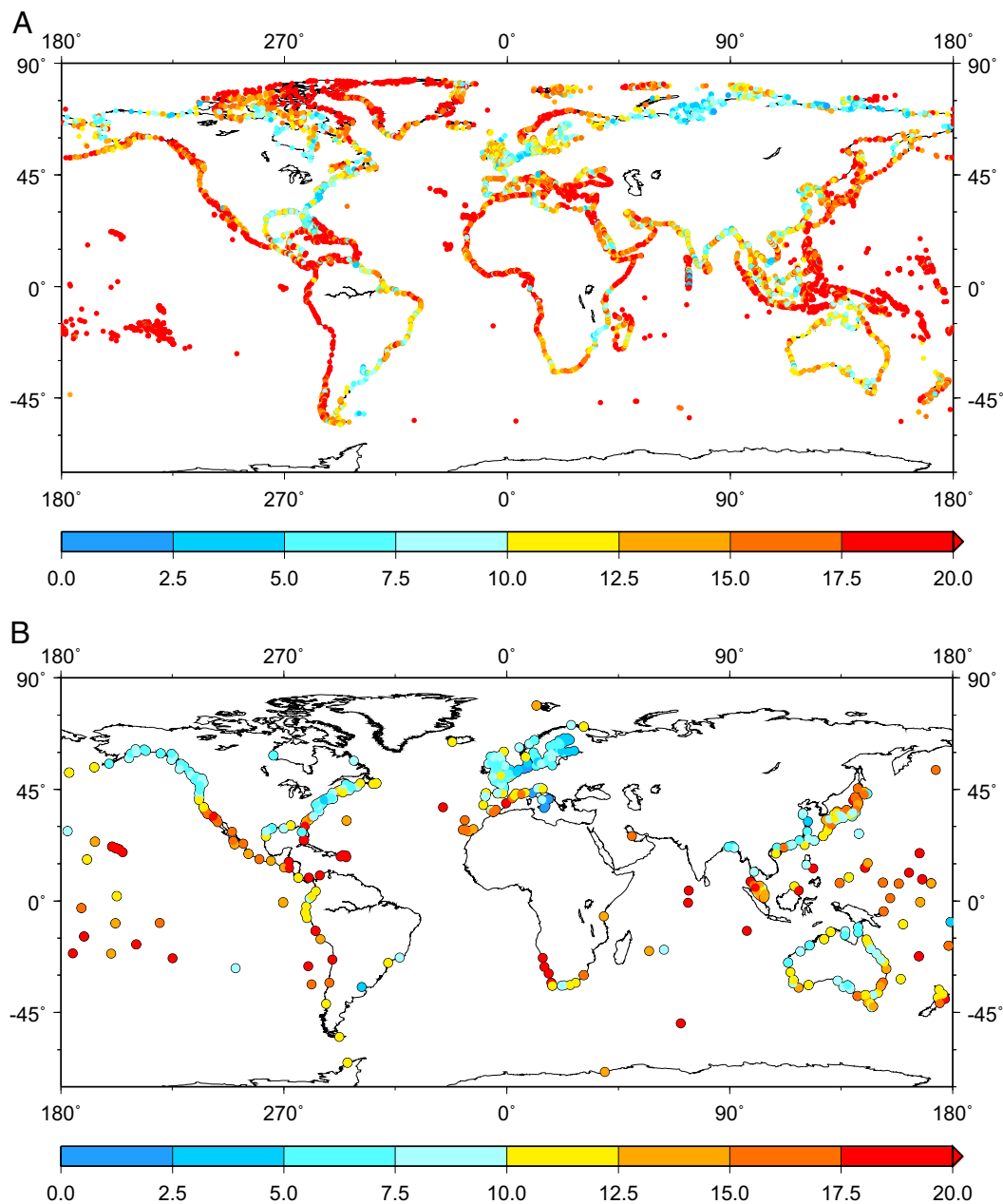
Fig. 3. Reciprocal (m^{-1}) of the Gumbel scale parameter (a) at each point on the world coastline in the D-C data set using $H1$ and $H100$ to compute the scale parameters, and (b) for records in GESLA-2 with at least 20 years of data.

correlation coefficient of 0.284. At a CCDF value of 0.5, the spread of the D-C curves is 0.59 m, and that of the GESLA-2 curves is 0.86 m.

It can be seen that Fig. 5(c) allows us to make both of our general points, but in terms of the overall distribution of data rather than at individual locations: the D-C information contains sets of $H1$–$H1000$ values that on average are too large and with return level curves that are too 'flat' when compared to GESLA-2 observations.

4. Effects on flood impacts at major coastal cities

As mentioned above, the point estimates of return water levels that we obtain from GESLA-2 cannot replace the D-C data in global impact models, such as DIVA, to explore the effects of the improved representation of extreme sea levels on exposure and risk estimates. However, we can use our results and perform such analyses for a selection of large coastal cities using the model developed by Hallegatte et al. (2013; hereafter H13). In H13, present-day and future (under sea

level rise and socio-economic scenarios) flood exposure and risk were assessed for the world's largest 136 port cities; extreme sea levels were taken from the D-C data set, as described above. Comparing the locations of these cities with those of the 655 tide gauges with more than 20 years of data in GESLA-2, we find that 59 (out of the 136) cities have a tide gauge within 200 km (Fig. 6). Hence, for these 59 cities we can quantify the effects of the discrepancies between D-C and GESLA-2 on present-day and future exposure and risk estimates.

There will undoubtedly be differences between D-C and GESLA-2 due to the fact that cities and tide gauges are not exactly collocated. We have analysed the Gumbel parameters for all pairs of GESLA-2 tide gauges that are within 200 km of each other, and find that the median differences in the location and scale parameters are 0.15 and 0.018 m, respectively (we quote the medians because the distributions of the differences are highly skewed). We believe that these differences are small compared with the discrepancies between D-C and GESLA-2 reported here.
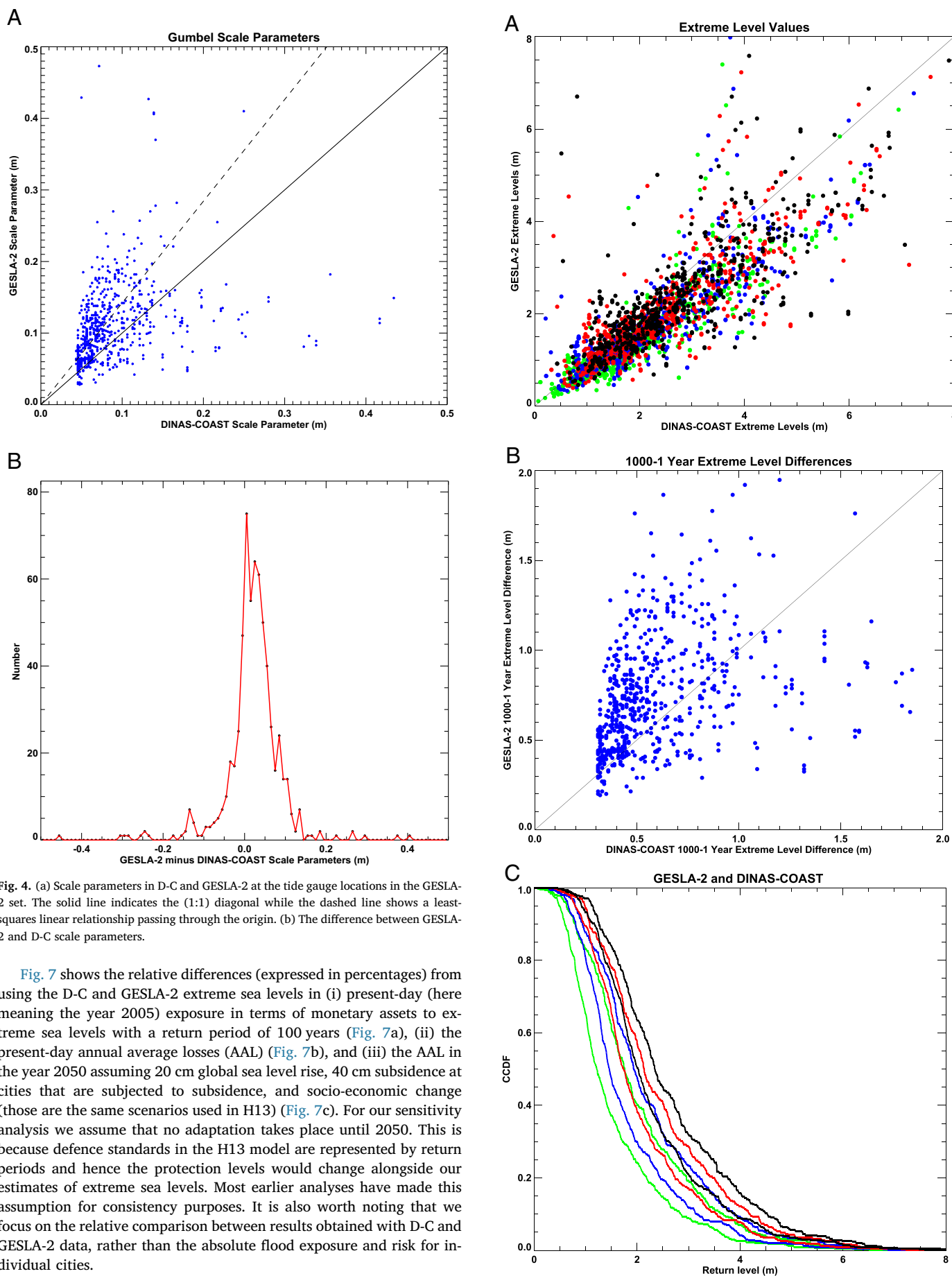
A Gumbel Scale Parameters

B

Fig. 4. (a) Scale parameters in D-C and GESLA-2 at the tide gauge locations in the GESLA-2 set. The solid line indicates the (1:1) diagonal while the dashed line shows a least-squares linear relationship passing through the origin. (b) The difference between GESLA-2 and D-C scale parameters.

A Extreme Level Values

B 1000-1 Year Extreme Level Differences

C GESLA-2 and DINAS-COAST

Fig. 7 shows the relative differences (expressed in percentages) from using the D-C and GESLA-2 extreme sea levels in (i) present-day (here meaning the year 2005) exposure in terms of monetary assets to extreme sea levels with a return period of 100 years (Fig. 7a), (ii) the present-day annual average losses (AAL) (Fig. 7b), and (iii) the AAL in the year 2050 assuming 20 cm global sea level rise, 40 cm subsidence at cities that are subjected to subsidence, and socio-economic change (those are the same scenarios used in H13) (Fig. 7c). For our sensitivity analysis we assume that no adaptation takes place until 2050. This is because defence standards in the H13 model are represented by return periods and hence the protection levels would change alongside our estimates of extreme sea levels. Most earlier analyses have made this assumption for consistency purposes. It is also worth noting that we focus on the relative comparison between results obtained with D-C and GESLA-2 data, rather than the absolute flood exposure and risk for individual cities.

(caption on next page)

In Fig. 7(a) and (b) we can see that the average absolute differences for the present-day 100-year exposure and AAL are in the order of 20% and 30%, respectively. Using D-C data leads to an overestimation of both exposure and AAL at most cities, but coherent underestimation for cities in Europe, the only region where D-C extreme sea levels are generally too low. When we include sea level rise (Fig. 7c) and assume no adaptation, the overestimation in AAL almost doubles to 57% and occurs consistently in all regions. There are two notable exceptions in Australia (Brisbane and Sydney), where the scale parameters obtained from the D-C levels are larger than the ones from GESLA-2 (i.e. the Gumbel distributions from D-C have a steeper slope).

The above analysis shows us the overall effects of improving the representation of extreme sea level for the exposure and risk analysis. As outlined in the previous sections, there are different types of discrepancies between the D-C and GESLA-2 data, namely differences in the location parameters (leading to offsets in the return levels) and differences in the scale parameters (leading to different slopes of the distributions). In order to quantify the effects of each of these discrepancies, we modify the Gumbel distributions that we obtain from the GESLA-2 data. We start by removing the vertical offset, which means that at a particular site we move the GESLA-2 distribution upwards or downwards so that the 10-year return levels match the ones from the D-C data (we did the same for the 1-year events and the results were essentially the same). We then use the modified distributions and extreme sea level information to repeat the exposure and risk analysis (Fig. 8a–c); this shows us the effect from having different slopes only. The differences in present-day 100-year exposure and AAL become much smaller (5% and 10% mean absolute differences) and now the D-C data leads generally to smaller values. This makes sense given that the modified distributions from GESLA-2 still have steeper slopes (at most sites) resulting in higher levels for long return periods (which are most important given that many cities have relatively high protection standards). Accordingly, there is still a significant over-estimation of close to 50% when using D-C extremes and adding sea level rise; this is predominantly due to differences in the scale parameters (or distribution slopes).
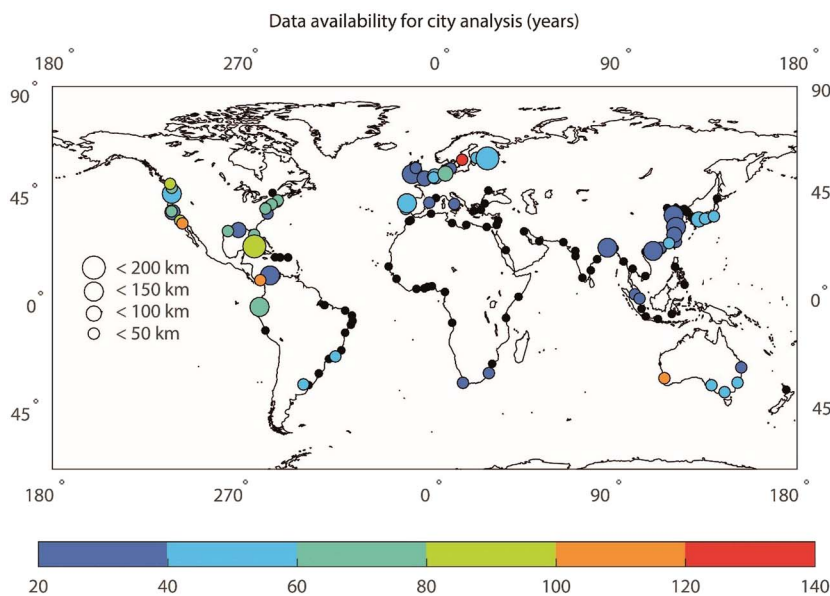
Next, we go back to our original distributions obtained from the GESLA-2 data and this time we modify their slope to match the ones obtained from the D-C data. To achieve this, the distributions are rotated about the 1-year return period values. We then again repeat the exposure and risk analysis in order to quantify the effect from having only vertical offsets in the distributions (Fig. 9a–c). For the present-day conditions the differences become much larger again (20% and 26% for 100-year exposure and AAL, respectively) and similar to those we found from the overall comparison (Fig. 7), but the mean absolute difference for AAL with sea level rise drops by almost half to 25%.
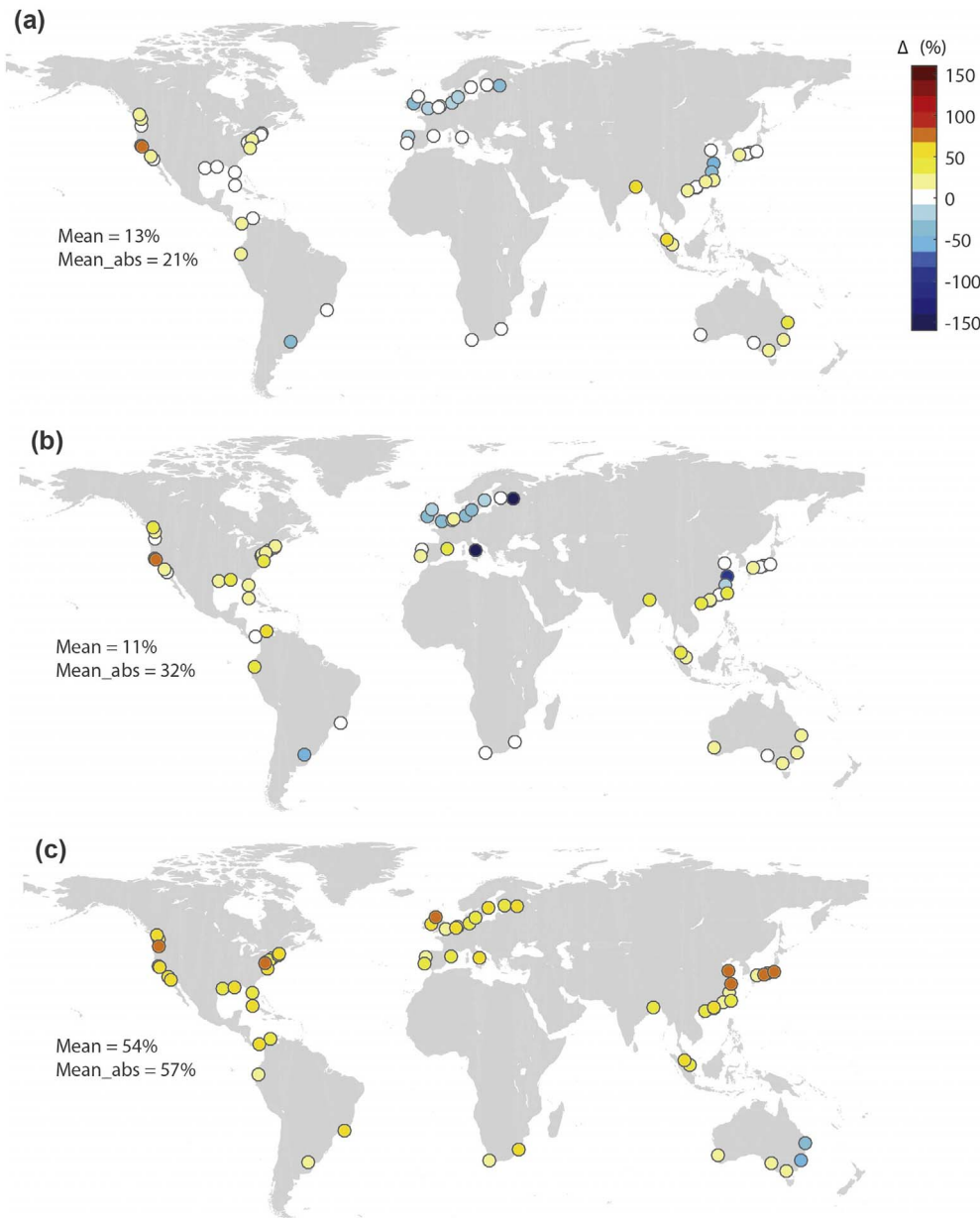
Based on these results we can make our third general point: that for present-day exposure and risk assessments, vertical offsets in the distributions (as defined by the 10-year return levels) are more important than discrepancies in the slopes, but when sea level rise is included discrepancies in the scale parameters (or slopes of the distributions) clearly dominate in terms of distorting results using the methods of H13, which are a standard approach for impact and risk models.

Despite the quantitative differences in 100-year exposure and AAL estimates, the absolute impacts remain significant and the ranking of the cities that are most exposed and at risk from coastal flooding changes little. Fig. SM4 shows the ranking according to present-day AAL when using D-C and GESLA-2 extremes. There is little change in the top 10 or top 20 of the 59 cities we were able to analyse. Hence, the overall conclusions found here remain consistent with the insights presented in H13.

5. Implications for extreme sea level frequencies with sea level rise

Why do these differences between D-C and GESLA-2 matter? This can be answered by inspection of Fig. 10(a) which shows the increase in the frequency of extreme sea levels around the world if MSL rises by 0.5 m, assuming that all other factors (tides, climatology of storm surges etc.) remain the same in the future, and therefore that scale parameters remain the same. Such a rise in MSL over the next 100 years is entirely plausible according to the IPCC AR5 (Church et al., 2013).

Fig. 10(a) was made using D-C scale parameters derived using Eq. (2). A Gumbel distribution will then imply an increase of $\exp\left(\frac{0.5}{\lambda}\right)$ in the frequency of a given level being exceeded for an 0.5 m MSL rise, with λ also in metres. It can be understood from this simple relationship why we chose to plot in Fig. 3 the reciprocal of the scale parameter, as the quantity of most interest, rather than the scale parameter itself. In addition, it can be seen that, given a typical scale parameter of 0.1 m and

Data availability for city analysis (years)

Fig. 6. Data availability (the colour bar indicating the number of annual maxima) at sites where tide gauges are located close (see size of circles) to cities analysed by Hallegatte et al. (2013); black dots denote cities where no tide gauges are close by or do not provide sufficient data (see text).

Fig. 7. Relative differences in (a) exposure of monetary assets to a 100-year extreme sea level event, (b) annual average losses under 2005 conditions, and (c) annual average losses for 2050 with sea level rise and no adaptation when using GESLA-2 and D-C extreme estimates; blue indicates that results based on D-C are too small, red means they are too high. Relative differences are expressed as (Value using D-C minus Value using GESLA) / Value using D-C.

an MSL rise of 0.5 m, then the increase in the frequency will be of the order of 150, and at locations where scale parameters are only a few centimetres (such as at some tropical islands or even at locations in the Mediterranean where the tidal range is small) almost any rise in MSL will lead to an extremely large increase in this frequency, and hence in the likelihood of flooding.

Fig. 10(b) shows the corresponding distribution using the GESLA-2 information. This figure provides an update to Fig. 13.25(a) in the IPCC AR5 and can be regarded as a set of 'true' values by means of which the worldwide distribution of Fig. 10(a) can be validated. In fact, major differences can be seen between (a) and (b). The ratios of the increases in frequency from D-C compared to those using GESLA-2 information are shown in Fig. 10(c), while their differences shown in Fig. SM3 yield almost the same conclusion. Fig. 10(c) and SM3 demonstrate in different ways that most coastlines would experience an increase in the likelihood of flooding (given an MSL rise of 0.5 m) that is much larger using D-C information than when using information from GESLA-2. This is also seen in the results from the city exposure and risk analysis for present-day and with future sea level rise.

6. Discussion and conclusions

We have undertaken a validation of the extreme sea level information in the DINAS-COAST data set by means of comparison with information obtained from the tide gauge records in the GESLA-2 data set, and we have explored the implications for flood impact studies. Our three main points are:

(1) The extreme levels in D-C are systematically too 'flat' (i.e. they do not increase with return period as fast as the GESLA-2 observations).
(2) The extreme levels in D-C (i.e. the H values) are systematically larger than those in the GESLA-2 observations.
(3) Differences (or uncertainties) in overall levels are more important for present-day exposure and impact analysis, but differences in scale parameters dominate when future sea level rise is included.

Point 2 suggests that the D-C approach modelled either the extreme tide and/or storm surge components of extreme sea levels inadequately. One could definitely argue that using MHW will not represent the tidal
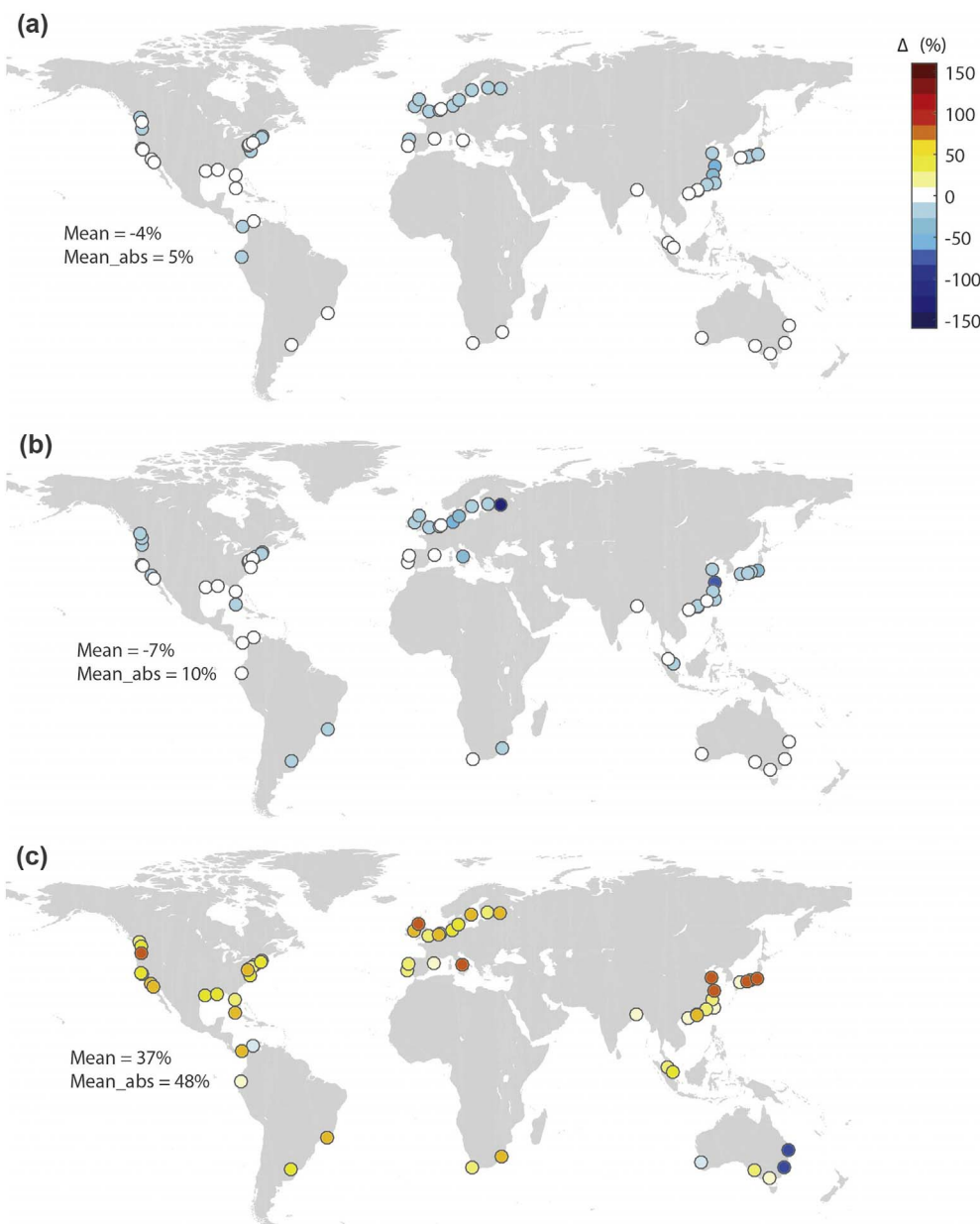
(a)

Mean = -4%
Mean_abs = 5%

(b)

Mean = -7%
Mean_abs = 10%

(c)

Mean = 37%
Mean_abs = 48%

Fig. 8. Same as Fig. 7, but the GESLA-2 offsets for 10-year return levels were removed to match the D-C results.

extremes adequately. Mean high water springs (MHWS) would have been a better choice, and would have been as easily accessible a quantity to extract from tide tables as MHW. However, parameterising the tidal extremes by MHW or MHWS does not allow nodal and peri-gean tidal variations to be included in the extremes; this will be one reason why the D-C extreme levels are too flat.

However, using these arguments concerning inadequacies in the tidal extremes would also lead one to the conclusion that the extreme levels in D-C are too low on average, rather than too high, as the GESLA-2 data shows (i.e. Point 2). Consequently, we suspect that the main reason that the D-C H values are too high stems from the way that the storm surge contributions were computed.

The main consequence of having $H1$ to $H1000$ values that are too high (relative to MSL) is that the present-day impact of flooding using a coastal database, in which heights are referred to a datum of MSL, will be over-estimated; see our results from the city analysis. However, when coastal defences and wider adaptation are considered, the situation is made more complex.

The main consequence of Point 1 is on studies of the change in likelihood of flooding when MSL rises. Using the D-C data will

overestimate the future growth in flood risk; for the cities we analysed here there is an overestimation of more than 50%. Of course, this topic only considers one component of impact and risk assessment (e.g. in our analysis we assume that no adaptation occurs). Nevertheless, sea level extremes are an important component of such analyses.

Point 3 highlights that efforts should be undertaken to remove off-sets and other biases from the various representations of extreme sea level information such as in D-C (and for the newer ones based on tide, surge and wave modelling mentioned below), in order to improve the quality of present-day risk analyses; the new GESLA-2 data base can provide helpful insights on where such biases exist and are most im-portant. In particular, when the impacts of sea level rise are being considered, it is important that the variability of extreme events is re-presented accurately in order to obtain a realistic slope to the extreme value distribution (which, in our case, was a Gumbel but which would be true for other parameterisations such as the GEV).

Overall, we have demonstrated that the improved data on sea level extremes from GESLA-2 clearly point in the direction of obtaining lower estimates than those obtained in previous studies for the exposure of people and assets to floods both today and in the future. An exploration
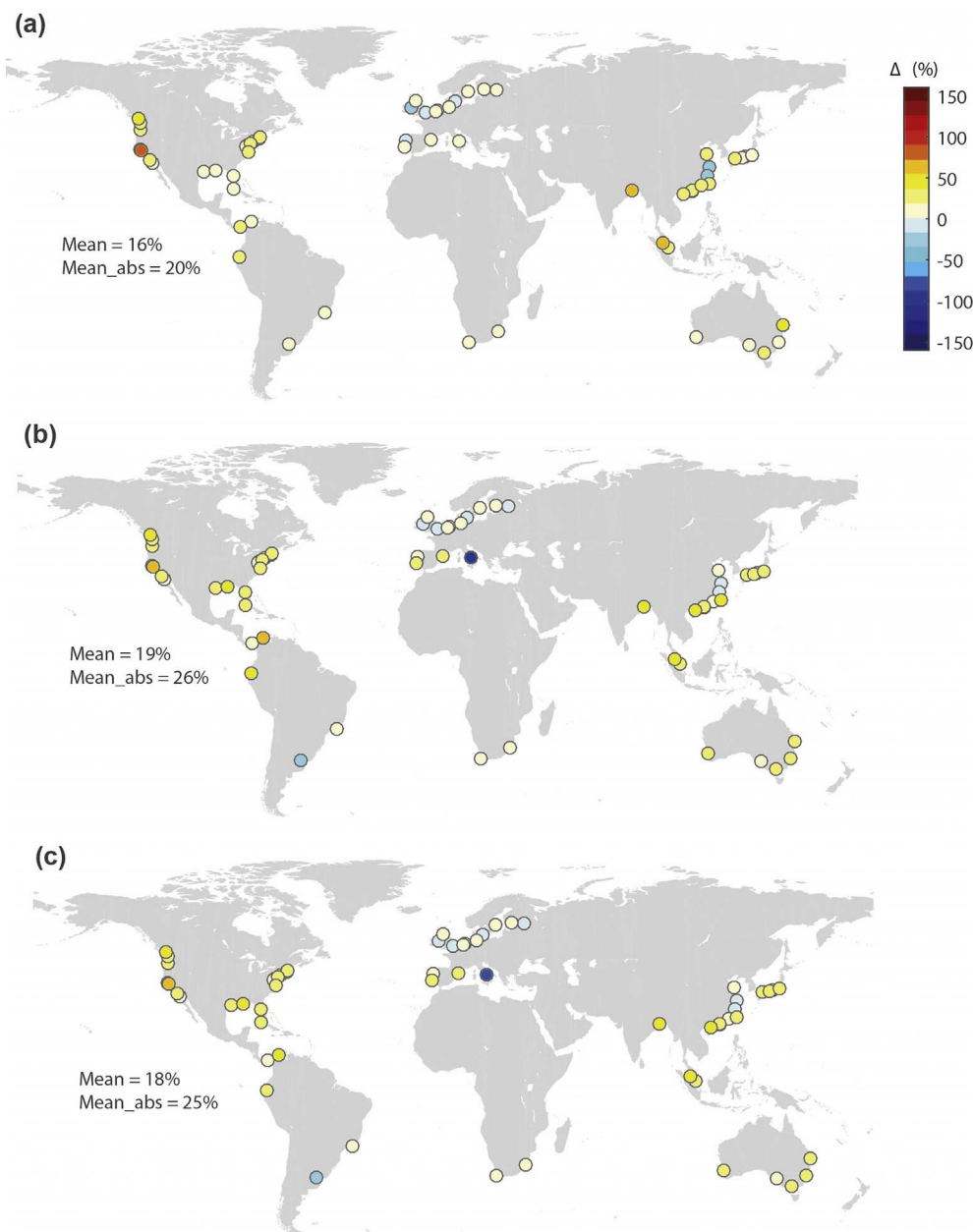
(a)

(b)

(c)

Fig. 9. Same as Fig. 7, but the slopes in the GESLA-2 return level estimates were adjusted to match the D-C results.

of the H13 results suggests that, while their estimates of impacts will need to be reduced, the insights and overall conclusions that emerge from that analysis are qualitatively robust. Of course, there is continuing interest in obtaining firmer estimates of actual losses and adaptation costs. However, the latter in particular are complex to calculate, which is why they have not been re-assessed in this paper.

Fortunately, improvements in large- to global-scale numerical modelling and related studies are allowing this to happen as illustrated by Muis et al. (2016), Vousdoukas et al. (2016) and other ongoing research, and by local studies of inundation probabilities and coastal impacts such as the modelling of the Gulf of Mexico by Bilskie et al. (2014). As these datasets on extremes become available, it is important that they be validated against a tide gauge data set such as GESLA-2, before being applied to new assessments that consider extreme sea levels with the other drivers of risk and exposure. In particular, it will be interesting to understand how an improved representation of extreme sea levels affects adaptation costs. As Wong et al. (2014) demonstrated, the costs of adaptation to sea level rise, particularly by developing countries, potentially represent enormous national investments: these

assessments should be updated for the next IPCC assessment. Given the agreement at the Conference of Parties (COP)-21 in Paris in December 2015 to limit global warming to 2° (and if possible to 1.5°), a focus on hotspots for coastal impacts and adaptation needs, such as small islands and deltas would be especially important.

Supplementary data to this article can be found online at http://dx.doi.org/10.1016/j.gloplacha.2017.06.007.
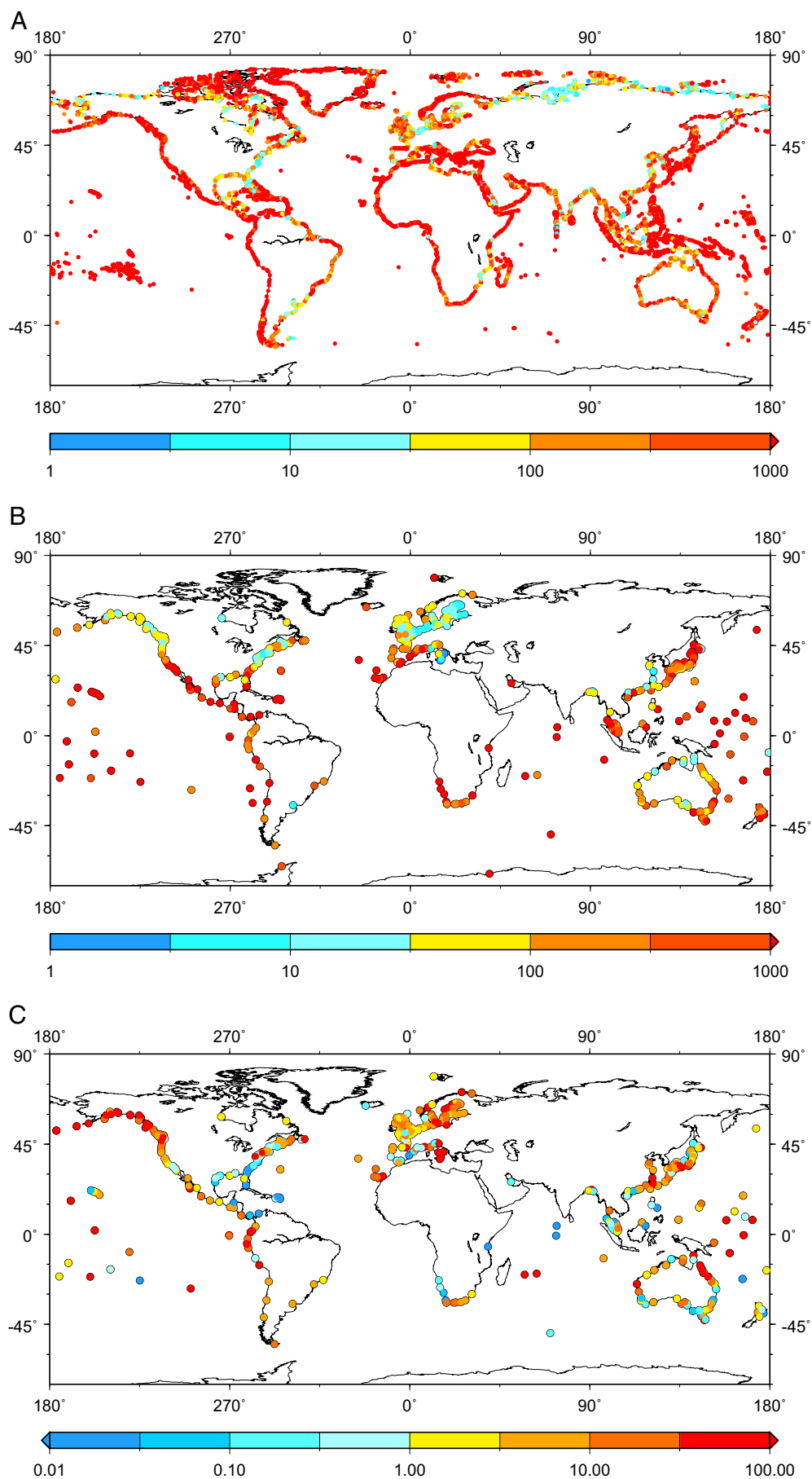
Fig. 10. Increases in the frequency of extreme sea levels if mean sea level rises by 0.5 m using (a) D-C and (b) GESLA-2 information. The colour scales saturate at 1000 for consistency with Fig. 13.25(a) of Church et al. (2013). (c) Ratio of the increases in frequency for D-C and those for GESLA-2, under 0.5 m of mean sea level rise.

References

Bilskie, M.V., Hagen, S.C., Medeiros, S.C., Passeri, D.L., 2014. Dynamics of sea level rise and coastal flooding on a changing landscape. Geophys. Res. Lett. 41, 927–934. http://dx.doi.org/10.1002/2013GL058759.

Bosello, F., Nicholls, R.J., Richards, J., Roson, R., Tol, R.S.J., 2012. Economic impacts of climate change in Europe: sea-level rise. Clim. Chang. 112, 63–81. http://dx.doi.org/10.1007/s10584-011-0340-1.

van den Brink, H.W., Können, G.P., 2011. Estimating 10000-year return values from short time series. Int. J. Climatol. 31 (1), 115–126. http://dx.doi.org/10.1002/joc.2047.

Brown, S., Nicholls, R.J., Lowe, J.A., Hinkel, J., 2016. Spatial variations of sea-level rise and impacts: an application of DIVA. Clim. Chang. 134, 403–416. http://dx.doi.org/10.1007/s10584-013-0925-y.

Church, J.A., Clark, P.U., Cazenave, A., Gregory, J.M., Jevrejeva, S., Levermann, A., Merrifield, M.A., Milne, G.A., Nerem, R.S., Nunn, P.D., Payne, A.J., Pfeffer, W.T., Stammer, D., Unnikrishnan, A.S., 2013. Sea Level change. In: Stocker, T.F., Qin, D., Plattner, G.-K., Tignor, M., Allen, S.K., Boschung, J., Nauels, A., Xia, Y., Bex, V., Midgley, P.M. (Eds.), Climate Change 2013: The Physical Science Basis. Contribution of Working Group I to the Fifth Assessment Report of the Intergovernmental Panel on Climate Change. Cambridge University Press, Cambridge, United Kingdom and New York, NY, USA.

Coles, S., 2001. An Introduction to Statistical Modeling of Extreme Values. Springer, London (208 pp).

Diaz, D.B., 2016. Estimating global damages from sea level rise with the Coastal Impact and Adaptation Model (CIAM). Clim. Chang. 137–143. http://dx.doi.org/10.1007/s10584-016-1675-4.

Hallegatte, S., Green, C., Nicholls, R.J., Corfee-Morlot, J., 2013. Future flood losses in major coastal cities. Nat. Clim. Chang. 3, 802–806. http://dx.doi.org/10.1038/NCLIMATE1979.

Hanson, S., Nicholls, R., Ranger, N., Hallegatte, S., Corfee-Morlot, J., Herweijer, C., Chateau, J., 2011. A global ranking of port cities with high exposure to climate extremes. Clim. Chang. 104, 89–111. http://dx.doi.org/10.1007/s10584-010-9977-4.

Hinkel, J., Klein, R.J.T., 2009. Integrating knowledge to assess coastal vulnerability to sea-level rise: the development of the DIVA tool. Glob. Environ. Chang. 19 (3), 384–395. http://dx.doi.org/10.1016/j.gloenvcha.2009.03.002.

Hinkel, J., Nicholls, R.J., Vafeidis, A.T., Tol, R.S.J., Avagianou, T., 2010. Assessing risk of and adaptation to sea-level rise in the European Union: an application of DIVA. Mitig. Adapt. Strateg. Glob. Chang. 15 (7), 703–719. http://dx.doi.org/10.1007/s11027-010-9237-y.

Hinkel, J., Lincke, D., Vafeidis, A.T., Perrette, M., Nicholls, R.J., Tol, R.S.J., Marzeion, B., Fettweis, X., Ionescu, C., Levermann, A., 2014. Coastal flood damage and adaptation costs under 21st century sea-level rise. Proc. Natl. Acad. Sci. 111, 3292–3297. http://dx.doi.org/10.1073/pnas.1222469111.

Hoozemans, F.M.J., Marchand, M., Pennekamp, H.A., 1993. A Global Vulnerability Analysis: Vulnerability Assessment for Population, Coastal Wetlands and Rice Production on a Global Scale, 2nd Edition. Delft Hydraulics, Delft, The Netherlands.

Hunter, J., 2012. A simple technique for estimating an allowance for uncertain sea-level rise. Clim. Chang. 113, 239–252. http://dx.doi.org/10.1007/s10584-011-0332-1.

Khouakhi, A., Villarini, G., 2016. Attribution of annual maximum sea levels to tropical cyclones at the global scale. Int. J. Climatol. http://dx.doi.org/10.1002/joc.4704.

McLeod, E., Hinkel, J., Vafeidis, A.T., Nicholls, R.J., Harvey, N., Salm, R., 2010. Sea-level rise vulnerability in the countries of the Coral Triangle. Sustain. Sci. 5 (2), 207–222. http://dx.doi.org/10.1007/s11625-010-0105-1.

Menéndez, M., Woodworth, P.L., 2010. Changes in extreme high water levels based on a quasi-global tide-gauge dataset. J. Geophys. Res. 115, C10011. http://dx.doi.org/10.1029/2009JC005997.

Merrifield, M.A., Genz, A.S., Kontoes, C.P., Marra, J.J., 2013. Annual maximum water levels from tide gauges: contributing factors and geographic patterns. J. Geophys. Res. Oceans 118, 2535–2546. http://dx.doi.org/10.1002/jgrc.20173.

Muis, S., Verlaan, M., Winsemius, H.C., Aerts, J.C.J.H., Ward, P.J., 2016. A global re-analysis of storm surge and extreme sea levels. Nat. Commun. 7, 1–11. http://dx.doi.org/10.1038/ncomms11969.

Nicholls, R.J., 2010. Impacts of and responses to sea-level rise. In: Church, J.A., Woodworth, P.L., Aarup, T., Wilson, W.S. (Eds.), Understanding Sea-level Rise and Variability. Chichester, UK, Wiley-Blackwell, pp. 17–51.

Nicholls, R.J., Hoozemans, F.M.J., 2005. Global vulnerability analysis. In: Schwartz, M. (Ed.), Encyclopaedia of Coastal Science. Kluwer Academic Publishers, Dordrecht, Netherlands, pp. 486–491. link.springer.com/referencework/10.1007%2F1-4020-3880-1.

Nicholls, R.J., Marinova, N., Lowe, J.A., Brown, S., Vellinga, P., de Gusmo, D., Hinkel, J., Tol, R.S.J., 2011. Sea-level rise and its possible impacts given a 'beyond 4C world' in the twenty-first century. Phil. Trans. R. Soc. A 369, 161–181. http://dx.doi.org/10.1098/rsta.2010.0291.

Pardaens, A.K., Lowe, J.A., Brown, S., Nicholls, R.J., de Gusmo, D., 2011. Sea-level rise and impacts projections under a future scenario with large greenhouse gas emission reductions. Geophys. Res. Lett. 38, L12604. http://dx.doi.org/10.1029/2011GL047678.

Pugh, D., Woodworth, P., 2014. Sea-level Science: Understanding Tides, Surges, Tsunamis and Mean Sea-level Changes. Cambridge University Press, Cambridge (ISBN 978-1-107-02819-7. 395 pp).

R Development Core Team, 2011. R: A Language and Environment for Statistical Computing. R Foundation for Statistical Computing, Vienna, Austria. http://www.R-project.org (ISBN 3-900051-07-0).

von Storch, H., Woth, K., 2008. Storm surges: perspectives and options. Sustain. Sci. 3, 33–43. http://dx.doi.org/10.1007/s11625-008-0044-2.

Vafeidis, A.T., Nicholls, R.J., McFadden, L., Tol, R.S.J., Hinkel, J., Spencer, T., Grashoff, P.S., Boot, G., Klein, R.J.T., 2008. A new global coastal database for impact and vulnerability analysis to sea-level rise. J. Coast. Res. 24 (4), 917–924. http://dx.doi.org/10.2112/06-0725.1.

Vousdoukas, M.I., Voukouvalas, E., Mentaschi, L., Dottori, F., Giardino, A., Bouziotas, D., Bianchi, A., Salamon, P., Feyen, L., 2016. Developments in large-scale coastal flood hazard mapping. Nat. Hazards Earth Syst. Sci. 16, 1841–1853. http://dx.doi.org/10.5194/nhess-16-1841-2016.

Wessel, P., Smith, W.H.F., 1998. New, improved version of Generic Mapping Tools released. EOS, Trans. AGU 79, 579.

Wolff, C., Vafeidis, A.T., Lincke, D., Marasmi, C., Hinkel, J., 2016. Effects of scale and input data on assessing the future impacts of coastal flooding: an application of DIVA for the Emilia-Romagna coast. Front. Mar. Sci. 3, 41. http://dx.doi.org/10.3389/fmars.2016.00041.

Wong, P.P., Losada, I.J., Gattuso, J.-P., Hinkel, J., Khattabi, A., McInnes, K.L., Saito, Y., Sallenger, A., 2014. Coastal systems and low-lying areas. In: Field, C.B., Barros, V.R., Dokken, D.J., Mach, K.J., Mastrandrea, M.D., Bilir, T.E., Chatterjee, M., Ebi, K.L., Estrada, Y.O., Genova, R.C., Girma, B., Kissel, E.S., Levy, A.N., MacCracken, S., Mastrandrea, P.R., White, L.L. (Eds.), Climate Change 2014: Impacts, Adaptation, and Vulnerability. Part A: Global and Sectoral Aspects. Contribution of Working Group II to the Fifth Assessment Report of the Intergovernmental Panel on Climate Change. Cambridge University Press, Cambridge, United Kingdom and New York, NY, USA, pp. 361–409.

Woodworth, P.L., Hunter, J.R., Marcos, M., Caldwell, P., Menéndez, M., Haigh, I., 2017. Towards a global higher-frequency sea level data set. Geosci. Data J. 3, 50–59. http://dx.doi.org/10.1002/gdj3.42.